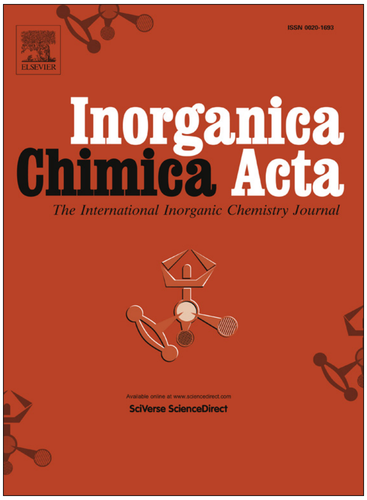

A New Terpyridine Cobalt Complex Redox Shuttle for Dye-Sensitized Solar Cells

Paolo Salvatori, Gabriele Marotta, Antonio Cinti, Edoardo Mosconi, Mallika Panigrahi, Lingamallu Giribabu, Mohammad K. Nazeeruddin, Filippo De Angelis

PII: S0020-1693(13)00374-5
DOI: http://dx.doi.org/10.1016/j.ica.2013.07.003
Reference: ICA 15546

To appear in: *Inorganica Chimica Acta*

Received Date: 6 May 2013
Revised Date: 26 June 2013
Accepted Date: 2 July 2013

Please cite this article as: P. Salvatori, G. Marotta, A. Cinti, E. Mosconi, M. Panigrahi, L. Giribabu, M.K. Nazeeruddin, F.D. Angelis, A New Terpyridine Cobalt Complex Redox Shuttle for Dye-Sensitized Solar Cells, *Inorganica Chimica Acta* (2013), doi: http://dx.doi.org/10.1016/j.ica.2013.07.003

A New Terpyridine Cobalt Complex Redox Shuttle for Dye-Sensitized Solar Cells

Paolo Salvatori,[a,b] *Gabriele Marotta,* [a,b] *Antonio Cinti,* [a,b] *Edoardo Mosconi,*[a] *Mallika Panigrahi,*[c]
Lingamallu Giribabu,[c] *Mohammad K. Nazeeruddin* [d], *Filippo De Angelis* [a,*]

[a] Computational Laboratory for Hybrid/Organic Photovoltaics (CLHYO), Istituto CNR di Scienze e Tecnologie Molecolari (ISTM-CNR), Via elce di Sotto 8, I-06123, Perugia, Italy.

[b] Department of Chemistry, University of Perugia, Via elce di Sotto 8, I-06123, Perugia, Italy.

[c] Inorganic & Physical Chemistry Division, CSIR-Indian Institute of Chemical Technology, Hyderabad 500607, India.

[d] Laboratory for Photonics and Interfaces, Institute of Chemical Sciences and Engineering, School of basic Sciences, Swiss Federal Institute of Technology, CH - 1015 Lausanne, Switzerland.

Corresponding author: E-mail: filippo@thch.unipg.it , Tel: +39 0755855523, Address: Via elce di Sotto 8, I-06213, Perugia, Italy.

ABSTRACT

A new cobalt-terpyridine redox shuttle ([Co(Cl-phenyl-terpyridine)$_2$]$^{2+/3+}$) has been synthesized, characterized, computationally investigated and then tested in photovoltaic devices, in conjunction with the prototypical N719 and Z907 ruthenium dyes. Lower efficiency compared to the reference [Co(bpy)$_3$]$^{2+/3+}$ redox couple were obtained, probably due to increased recombination processes. Improvements in the devices performances were obtained by using chenodeoxycholic acid as surface co-adsorbent and as an electrolyte additive. Moreover, to better rationalize the photovoltaic results, the effect of two different counterions (TFSI and PF$_6$) has been investigated for the reference [Co(bpy)$_3$] $^{2+/3+}$ electrolyte, finding a reduced efficiency for the TFSI-based electrolyte.

GRAPHICAL ABSTRACT

KEYWORDS: Dye-Sensitized Solar Cells (DSCs), Electrolyte, Cobalt complex, Terpyridine, Chenodeoxycholic acid.

1. Introduction

Dye-sensitized Solar Cells (DSCs) represent a promising approach to the direct conversion of sunlight into electrical energy at low cost and with high efficiency.[1-4] This has been very recently demonstrated by the launch of the first DSC-based commercial product. DSCs are based on a dye-sensitized mesoporous oxide layer, usually composed by a network of sintered nanoparticles (typically anatase TiO_2 ~20-30 nm diameter), interpenetrated by a liquid redox electrolyte (typically I^-/I_3^- or Co(II)/Co(III)-polypiridine complexes in a volatile organic solvent). Upon photoexcitation of the chemisorbed dye, charge separation occurs at the dye-sensitized semiconductor interface and electrons are injected into the oxide conduction band (CB); the generated charges travel across the TiO_2 nanoparticle network and can be collected at the transparent conducting glass back contact. The oxidized dye is regenerated by the redox shuttle electrolyte. The circuit is closed by electrolyte regeneration at the counter-electrode.

The DSCs efficiency is the product of the short-circuit photocurrent density (J_{sc}), the open circuit voltage (V_{oc}) and the cell fill-factor (FF) divided by the intensity of the incident light (I_s), namely:

$$\eta = J_{sc} \times V_{oc} \times FF / I_s \qquad (1)$$

The photocurrent density is directly related to the charge generation and collection efficiency, which in turn depend upon the dye light-harvesting and the kinetics of electron injection, dye regeneration and charge transport within the cell. As such, a sizable contribution to J_{sc} depends directly on the dye. The DSCs open circuit voltage represents the difference between the quasi-Fermi level of the semiconductor under illumination and the redox potential of the redox shuttle electrolyte, the latter being nearly constant under operation conditions due to the high concentration of redox species. The quasi-Fermi level ($E_{F,n}$) of the semiconductor depends “statically” on the semiconductor conduction band (CB) energy and “dynamically” on the charge density (n) accumulated in the semiconductor,[5] according to the following equation:

$$E_{F,n}=E_{CB}+k_BT\ \ln[n/N_c] \qquad (2)$$

where N_c is the density of states in the semiconductor. A higher semiconductor CB and charge density accumulation in the semiconductor provide a raise of the quasi-Fermi level and thus of the V_{oc}. A more positive redox shuttle potential also leads to an increased V_{oc}. This is exploited in Co(II)/Co(III) electrolytes and in general in transition metal redox shuttle endowed with a tunable redox potential.[6]

The I^-/I_3^- redox couple in an organic solvent has been considered as the standard high-performance electrolyte in DSCs for many years; all champion DSCs reported up to 2010 were based on such redox couple.[7, 8] Solid state DSCs based on molecular dyes and the spiro-OMeTAD solid hole conductor are also actively investigated, delivering top efficiencies of about 7%.[9, 10] The employment of lead perovskites as absorbers and hole conductors,[11-15] both in traditional TiO_2-based DSCs[11, 15-17] and in the recently proposed meso-superstructured solar cells[12, 18] has further boosted the efficiency of solid-state devices, with top efficiency exceeding 12%.[17, 18]

Although highly performing, the I^-/I_3^- redox couple has several disadvantages, including its high corrosivity towards most of noble metals, except gold, which imposes stringent requisites to DSCs module fabrication. Also, the unfavorable thermodynamics of its complex two-electron redox cycle implies DSCs voltage losses of ca. 600 mV,[19] mainly related to the dye regeneration process.[20] The two-electron / bimolecular nature of the recombination pathway between injected electrons and the oxidized dye or oxidized species in the electrolyte is a key to suppress such parasitic processes, which would reduce both V_{oc} and J_{sc}.[19, 21] Various attempts have been made to replace the I^-/I_3^- redox couple by alternative electrolytes based on simpler one-electron redox couples, although the high recombination rates typical of such systems has prevented for a long time to achieve high photovoltaic performances. Among the systems which have been experimented, we mention Co(II)/Co(III) polypiridyl complexes,[5, 22-31] Fe(II)/Fe(III) ferrocene/ferrocenium complexes,[9, 32-34] Cu(I)/Cu(II) complexes,[35, 36] organic redox couples,[37, 38] CuNCS[39, 40] and S^-/S_2^- redox couples, the latter being largely employed in quantum dot-based DSCs.[41-43] Very interestingly, the investigated transition metal complexes have tunable redox potentials which can be pushed up to ca. 1 V vs. SHE, so that if efficient charge collection can be achieved, a correspondingly higher V_{oc} might be extracted. Maintaining the same J_{sc} and FF of champion DSCs based on I^-/I_3^-, this readily translates into overall device efficiencies approaching 15%.

For one-electron redox shuttles, several promising results[22, 24, 31] have been obtained in combination with organic dyes. In particular, it was reported that the sterically congested D35 and Y123 organic dyes, used in conjunction with a $[Co(bpy\text{-}pz)_2]^{2+/3+}$ electrolyte, lead to photovoltaic efficiency of ~10%, with DSSCs open circuit voltage exceeding 1 V.[24] On the other hand, the prototypical high-efficiency Ru(II) N719 dye, Scheme 1, delivered dramatically low photovoltaic efficiency, ~2%, when using a Co(II)/Co(III) redox mediator,[5, 27] while the same system provided high efficiency exceeding 11% when coupled to the I_3^-/I^- redox couple.[44] Interestingly, not all Ru(II)-dyes performed poorly with Co(II)/Co(III) redox mediators; the Ru(II) Z907 dye, endowed with long nonyl chains, delivered similar efficiency with Co(II)/Co(III) (η = 6.5%) and with I_3^-/I^- redox couples (η = 7.7%).[5]

Scheme 1. Chemical structures of the ruthenium N719 and Z907 dyes.

The reason for this widely varying efficiency of DSCs employing Ru(II)-dyes and Co(II)/Co(III) electrolytes was investigated in our previous work[45] where the effective formation of a rather strong Ru(II)-Co(III) ion-pair between N719 and $[Co(bpy)_3]^{3+}$ was found leading to an high probability of intercepting TiO_2 – injected electrons by the oxidized $[Co(bpy)_3]^{3+}$ species, lying close to the N719-sensitized TiO_2 surface. Moreover, the good efficiency of Z907 with Co(II)/Co(III) electrolytes was associated to a surface-blocking effect, whereby the long alkyl dye chains would form a compact dye layer, impeding the close approach of the Co(III) species to the semiconductor surface.[5, 45] A similar effect explained the high performance of organic dyes with bulky substituents on the donor moiety.[22, 24, 31, 45] In both cases, shifting the distribution of Co(III) ions away from the semiconductor surface was demonstrated to be key for high efficiency.[45]

A further interesting aspect concerning Co(II)/Co(III) and Fe(II)/Fe(III) redox couples,[32] lies in the observation that including the prototype chenodeoxycholic acid (CDCA) co-adsorbent both in the dye *and* in the electrolyte solution substantially improved the DSCs performance, both in terms of V_{oc} and J_{sc}. [32, 46] This unprecedented observation seems to be the key to further expanding the applicability of alternative redox couples for high performance DSCs, in line with the reported use of supramolecular chemistry to control charge recombination and other reactions in DSCs, as detailed by Planells et al.[47, 48].

An interesting conclusion of our previous work concerned the mechanism of regeneration of the oxidized dye by the reduced Co(II) complex,[45] whereby a low-spin/high-spin equilibrium of the Co(II) ions seems to play a role in accessing fast regeneration rates, therefore high short-circuit photocurrent densities. A lower reorganization energy (λ) was calculated for the low-spin regeneration pathway, with bis-tridentate Co(II)/Co(III) complexes (e.g. terpyridine, Scheme 2) leading to a lower λ compared to tris-bidentate species (e.g. bipyridine-, Scheme 2, and phenanthroline-based cobalt complexes) both for the low spin and high spin pathways.[45] This observation prompted us to synthesize two substituted terpyridine Cobalt complexes based on commercially available ligands, i.e. 4’-(4-Chloro)-2,2’:6’,2’’-terpyridine (**Cl-terpy**) and a 4’-(4-Chlorophenyl)-2,2’:6’,2’’-terpyridine (**Cl-phen-terpy**). While this work was in progress, the synthesis and photovoltaic characterization of DSCs based on [Co(Cl-terpy)$_2$]$^{+2/+3}$ complexes was reported by Aribia et al.,[49] so we limited our attention to the novel [Co(Cl-phen- terpy)$_2$]$^{2+/3+}$ complexes, (Scheme 2).

Scheme 2. Chemical structures of the cobalt complexes (a) [Co(Cl-phen-terpy)$_2$]$^{2+/3+}$, and (b) [Co(bpy)$_3$]$^{2+/3+}$.

Here we thus report on the synthesis, characterization, computational analyses and photovoltaic measurements for DSCs based on the novel electrolyte in conjunction with Z907 and N719 ruthenium dyes, comparing our results to additional data obtained for the prototype [Co(bpy)$_3$]$^{2+/3+}$ electrolyte, for which we also tested the effect of two different counterions, i.e. **[PF$_6$]$^-$** and [Bis(trifluoromethane)-sulfonimide] **[TFSI]$^-$**. Our results confirm the beneficial effect of CDCA both in the dye solution and in electrolyte, that seems to be independent of the employed cobalt electrolyte. Lower performances were obtained with the new [Co(Cl-phen- terpy)$_2$](TFSI)$_{2/3}$ electrolyte compared to the reference [Co(bpy)$_3$]$^{2+/3+}$ system, possibly due to the high recombination losses and to the limited diffusion of the [TFSI]$^-$ counterions, that we used with the [Co(Cl-phen- terpy)$_2$]$^{2+/3+}$ complex for solubility reasons, observed by comparing the performances of the [Co(bpy)$_3$]$^{2+/3+}$ electrolytes with [TFSI]$^-$ and [PF$_6$]$^-$ counterions.

2. Experimental section

2.1 Materials

All the materials used in this work were used as received, without further purification, if not stated otherwise. The N719 and Z907 dyes the TiO_2 pastes and were purchased from Solaronix. Z907 dye powders were purified by using HPLC (Waters 996, equipped with a photodiode array detector). The dye powder was solubilized in ethanol and injected in the cromatographic column (Phenomenex Jupiter, 10µm, C18, 250mm x 21mm). The mobile phase consisted of distilled acetonitrile with 0.1% of trifluoroacetic acid (CF_3COOH).

Synthesis of [Co(Cl-phenyl-terpy)$_2$](TFSI)$_2$. 0.26 g of $CoCl_2*6H_2O$ (1.1 mmol) was dissolved in 15 ml of methanol. At this solution was added, under magnetic stirring and low heating (about 60°C), a solution of the ligand 4'-(4-Chlorophenyl)-2,2':6',2''-terpyridine (0.83g, 2.4 mmol, in 60 ml of ethanol). The resulting solution, colored in dark red-brown, was put at reflux at 70°C for 2 h. Then the precipitating reagent Bis(trifluoromethane)-sulfonimide lithium salt (LiTFSI), (0.69 g, 2.2 mmol, in 15 ml of ethanol was added to the solution. After that, the solution was again put at reflux for 30 minutes. After about 1 h, from the cooling solution, was separated a crystalline dark brown product of the complex of cobalt(II). Then the product was collected by filtration and washed several time with little amounts of ethanol. Finally the product was dried under vacuum at 60 °C. Elemental analysis Calculated for $C_{46}H_{28}N_8Cl_2O_8S_4F_{12}Co$: C, 42.28; H, 2.16; N, 8.57; Found C, 43.11; H, 1.98; N, 8.42.

Synthesis of [Co(Cl-phen-terpy)$_2$](TFSI)$_3$. A solution of $CoCl_2*6H_2O$ (0.25 g, 1.05mmol) in water was added to a methanolic solution of 4'-(4-Chlorophenyl)-2,2':6',2''-terpyridine (1.08 g, 3.15 mmol in 50 mL of methanol). The excess of ligand not fully solubilized was filtered. To the solution was then added a methanolic bromine solution (0.14g, 0.9mmol in 6ml) and immediately get some precipitate. The precipitate was separated and to the filtrate solution an excess of LiTFSI (0.98g, 3.4 mmol, in 10 ml of water) was added to get the precipitate of oxidized form of the cobalt complex. The precipitate was collected and washed with water and dried under vacuum to isolate

[Co(Cl-phen-tpy)$_2$](TFSI)$_3$. Elemental analysis: Calculated for $C_{48}H_{28}N_9Cl_2O_{12}S_6F_{18}Co$: C, 36.33; H, 1.78; N, 7.94; Found C, 36.26; H, 1.84; N, 7.69. The complex was further analyzed by NMR, Supplementary data.

Synthesis of [Co(bpy)$_3$](TFSI)$_2$. 2,38 g of **$CoCl_2$•6H_2O** (10 mmol) was dissolved in 15 ml of methanol. At this solution was added, under magnetic stirring and mild heating (about 60°C) , a solution attained by dissolving 5.14 g (33 mmol) of the ligand 2,2'bipyridine in 10 ml of ethanol. The resulting solution, clear brown colored, was put at reflux at 70°C for 2 h. Then to the solution was added the precipitating reagent, LiTFSI, through a solution attained by dissolving 6,32 g (22 mmols) of such salt in 15ml of ethanol. After that, the solution was again put at reflux for 30 minutes. After about 3 h, from the cooling solution, was separated a crystalline dark yellow product of the complex of cobalt(II). Then the product was collected by filtration and washed several time with little amounts of ethylic ether – ethanol solution (1:1). The collected product was dried under vacuum at 60°C. Elemental analysis: Calculated for $C_{34}H_{24}N_8O_8S_4F_{12}Co$: C, 37.55; H, 2.21; N, 10.30; Found C, 36.80; H, 2.18; N, 9.76.

Synthesis of [Co(bpy)$_3$](TFSI)$_3$. A solution of $CoCl_2$*6H_2O (0.50 g, 2.10mmol) in water was added to a methanolic solution of 2,2'bipyridine (1.09 g, 7.0 mmol). To the solution was then added a methanolic bromine solution (0.28g, 1.8mmol in 6ml) and immediately get some precipitate. The precipitate was separated and to the filtrate solution an excess of LiTFSI (2.02g, 7mmol, in 15 ml of water) was added to get the precipitate of oxidized form of the cobalt complex. The precipitate was collected and washed with water and dried under vacuum to isolate [Co(bpy)$_3$](TFSI)$_3$. Elemental analysis: Calculated for $C_{36}H_{24}N_9O_{12}S_6F_{18}Co$: C, 31.61; H, 1.75; N, 9.21; Found C, 34.30; H, 2.01; N, 9.35. The complex was further analyzed by NMR, Supplementary data.

The synthesis of the [Co(bpy)$_3$][PF$_6$]$_2$ and [Co(bpy)$_3$][PF$_6$]$_3$ complexes follows a standard route and is reported in our previous paper.[46]

2.2 Methods

^{1}H NMR and ^{19}F NMR spectra were measured on a Bruker DRX 400 spectrometer at 298.0 ± 0.1 K in acetonitrile solution.

The UV-Visible absorption spectra were recorded in acetonitrile solution on a Perkin-Elmer Lambda 800 spectrophotometer.

Cyclic voltammetry measurements were performed on a PC-controlled CH instruments model CHI 620C electrochemical analyzer in CH_3CN solvent at scan rate of 100 mV/s with 0.1 M tetrabutyl ammonium perchlorate (TBAP) as supporting electrolyte. The working electrode is glassy carbon, standard calomel electrode (SCE) is reference electrode and platinum wire is an auxiliary electrode.

2.3 Solar cells fabrication and characterization

FTO glass (TEC-15, 2.2 mm thickness, Solaronix) was used for transparent conducting electrodes. The substrate was first cleaned in a ultrasonic bath using a detergent solution, acetone and ethanol respectively (each step 15 min. long). The FTO glass plates were immersed into a 40 mM aqueous $TiCl_4$ solution at 70 °C for 30 min and washed with water and ethanol. A layer of opaque TiO_2 paste (Solaronix D-20) was spread on the FTO glass plates by doctor blade. The TiO_2 layer was treated in an ethanol chamber and dried for 5 min at 120°C. The TiO_2 coated electrodes (active area 0.2 cm^2) were gradually heated under air flow at 325 °C for 5 min, at 375 °C for 5 min, at 450 °C for 15 min, and 500 °C for 15 min. After the sintering process, the TiO_2 film was treated with 40 mM $TiCl_4$ solution, then rinsed with water and ethanol. The electrodes were heated at 500 °C for 30 min and after cooling (80 °C) were immersed for 20 hours into sensitizing baths. These consisted of EtOH solutions of the N719 and Z907 dyes (Solaronix) in 0.2 mM concentration, and when required with 20.0 mM of 3a,7a-dihydroxy-5b-cholic acid (CDCA) added. Counter electrodes were prepared by coating with a drop of H_2PtCl_6 solution (2 mg of Pt in 1 mL of ethanol) a FTO plate (TEC 15/2.2 mm thickness, Solaronix) and heating at 400 °C for 15 min. The TiO_2 sensitized photoanode and Pt counter electrode were assembled into a sealed sandwich-type cell by a hot-melt ionomer film (Surlyn, 25 μm thickness, Dyesol). The electrolyte solution was inserted by vacuum backfilling. Then, the hole was sealed by using additional Surlyn patch and a cover glass and finally a conductive Ag-based paint was deposed at the electrical contacts.

Three electrolyte solutions were prepared with the $[Co(bpy)_3][PF_6]_{2/3}$,$[Co(bpy)_3][TFSI]_{2/3}$ and $[Co(Cl\text{-}phen\text{-}terpy)_2][TFSI]_{2/3}$, according to the following composition: 0.2M [Co(II)], 0.02M [Co(III)], 0.1 M $LiClO_4$, and 0.5 M 4-tert-butylpyridine in acetonitrile. Where required, CDCA (Solaronix) was added to the electrolyte in 0.01M concentration. The reference I^-/I_3^- based electrolyte was the commercially available Iolitech ES-0004 HP, containing 1butyl-3methylimidiazolium iodide, iodine, guanidinium thiocyanate and *tert*-butylpyridine, in a mixture of valeronitrile and acetonitrile.

Photovoltaic measurements were recorded by means of AM 1.5 solar simulator equipped with a Xenon lamp (LOT-ORIEL LS 0106). The power of incoming radiation, set at 100 mW/cm^2, was checked by a piranometer. J–V curves were obtained by applying an external bias to the cell and measuring the generated photocurrent with a Keithley model 2400 digital source-meter, under the control of dedicated LabTracer 2.0 software. A black shading mask was employed to avoid the overestimation of the measured parameters.

2.4 Computational details

We performed geometry optimization in solution for the investigated series of cobalt complexes. Co(III) are calculated in a closed shell singlet, while for the Co(II) complexes both doublet (low-spin, LS) and quartet (high spin, HS) spin states were considered. The B3LYP hybrid functional[50] and solvation effects with the continuum polarizable model (PCM)[51] as implemented in the Gaussian09[52] package program. The 6-311G* basis set was used throughout this study. This computational approach has been already validated in our previous work.[45] The solution free energy between difference the oxidized and the reduced species was compared with the experimental oxidation potentials. Oxidation potentials measured against the NHE electrode were reported against the vacuum level set at -4.44 eV vs. NHE. Reorganization energies were calculated in solution, considering equilibrium solvation. This approach was shown to provide reorganization energy values in close agreement to experimental estimates.[30, 45]

3. Results and discussion

3.1 Electrochemical and optical properties

The $[Co(Cl\text{-}phen\text{-}terpy)_2][TFSI]_{2/3}$ complex shows a redox potential of 0.474 V vs. NHE (Figure 1), which is slightly less positive than the oxidation potential of the reference $[Co(bpy)_3]$ complex (0.56 V vs. NHE) [22] and is also less positive than the oxidation potential of the $[Co(Cl\text{-}terpy)_2][TFSI]_{2/3}$ complex (0.603 vs. NHE).[49] This can be rationalized by the screening effect of the intervening phenyl moiety which separates the terpyridine core from the electron-withdrawing chloride. The oxidation potential of the $[Co(Cl\text{-}phen\text{-}terpy)_2][TFSI]_2$ complex is however more positive than the standard I^-/I_3^- redox couple (0.35V vs NHE),[19] which could potentially increase the cells V_{oc}.

Figure 1. Cyclic voltammogram of $[Co(Cl\text{-}phen\text{-}terpy)_2](TFSI)_{2/3}$ in acetonitrile solution.

A comparison of calculated and experimental oxidation potentials for various relevant cobalt complexes is reported in Table 1. As it can be noticed, our calculated values are in good agreement with the corresponding experimental measurements, with a maximum deviation of 0.08 eV found for the $[Co(terpy)_2]^{2+/3+}$ system. It is also interesting to notice that in line with our previous work and with experimental data,[22, 45, 49, 53] the $[Co(bpy)_3]^{2+}$ complex shows a high-spin ground state, while the $[Co(R\text{-}terpy)_2]^{2+}$ complexes with R=H and Cl-phen show a low-spin ground state. Interestingly, our calculations indicate that the $[Co(Cl\text{-}terpy)_2]^{2+}$ complex shows a high-spin ground state, although with a reduced HS/LS energy splitting compared to the $[Co(bpy)_3]^{2+}$ complex. It has to be noticed that the present method of calculation tends to over-stabilize the HS state, so it is likely that also [Co(Cl-terpy)$_2$]$^{2+}$ complex could show a low-spin ground state, although with a reduced HS/LS energy difference compared to the clearly low-spin [Co(R-terpy)$_2$]$^{2+}$ complexes (R=H, Cl-phen).

Table 1. Comparison of calculated and experimental oxidation potentials (eV, vs. vacuum). Also reported are calculated HS-LS splitting and HS and LS reorganization energies (λ^{LS} and λ^{HS}) for the regeneration (REG) and recombination reaction (REC). All values are in eV.

Compound	**R**	**ΔE_{OX}**			**Co(II)→Co(III)**		**Co(III)→Co(II)**	
		Theor.	**Exp.**	**ΔE_{HS-LS}**	**λ^{LS}**	**λ^{HS}**	**λ^{LS}**	**λ^{HS}**
[Co(bpy)$_3$]$^{2+/3+}$	H	5.06	5.00[a]	-0.21	0.62	1.34	0.73	1.35
[Co(R-terpy)$_2$]$^{2+/3+}$	H	4.86	4.94[b]	+0.05	0.51	1.37	0.55	1.33
	Cl	5.10	5.07[c]	-0.12	0.51	1.51	0.65	1.52
	Cl-phen	4.87	4.91	+0.06	0.51	1.38	0.54	1.31

[a] Experimental value +4.44 from Ref.[22]; [b] from Ref.[54]; [c] from Ref. [49].

It is also interesting to notice that the series of [Co(R-terpy)$_2$]$^{2+}$ complexes show reduced reorganization energies for the low-spin regeneration/recombination pathways compared to the high-spin ones compared to the standard [Co(bpy)$_3$]$^{2+}$ complex. The high-spin values are on the other hand comparable or higher. This data thus confirms the design rule which led us to synthesize the present complex, i.e. to exploit a lower reorganization energy to speed up the regeneration of the oxidized dye by the Co(II) ions. We notice, however, that a lower reorganization energy is also calculated for the recombination with Co(III) ions, which could lead to potential losses in the DSCs.[55]

The lack of competition for the light absorption with the dye is one of the main advantages of the cobalt complexes with respect to the iodide-based electrolytes. The UV-Visible absorption spectra of the [Co(Cl-phen-terpy)$_2$](TFSI)$_{2/3}$ complexes in acetonitrile solution are reported in Figure 2. Both the reduced and oxidized complexes show their absorption maxima in the UV region, at 287 nm, with an extinction coefficient of respectively 69700 and 62300 mol/cm^{-1}/L^{-1}. In the visible region the Co(II) complex has a weak absorption feature (ε=2400 mol/cm^{-1}/L^{-1} at 517 nm), while for the oxidized complex we have only the tail of the UV-centered absorption band.

Figure 2. Absorption spectra of **[**Co-(Cl-phen-terpy)$_2$](TFSI)$_2$ (red line) and **[**Co-(Cl-phen-terpy)$_2$](TFSI)$_3$ (blue line) in acetonitrile.

3.2 Photovoltaic data

The photovoltaic parameters of DSCs using [Co(Cl-phen-terpy)$_2$](TFSI)$_{2/3}$ as electrolyte are reported in Table 2 and Figure 3, in comparison with [Co(bpy)$_3$](TFSI)$_{2/3}$ and [Co(bpy)$_3$](PF$_6$)$_{2/3}$ devices, made in the same fabrication conditions, used as a reference. For comparison, we also reported the photovoltaic parameters with a standard I$^-$/I$_3^-$ based commercial electrolyte (IOLITECH ES004-HP), representing our benchmark performances.

Table 2. Photovoltaic parameters of DSCs employing [Co(Cl-phen-terpy)$_2$](TFSI)$_{2/3}$, [Co(bpy)$_3$](TFSI)$_{2/3}$ (bpy-TFSI) and [Co(bpy)$_3$](PF$_6$)$_{2/3}$ (bpy-PF$_6$) based electrolyte. Measurements were made under simulated AM 1.5, 1 Sun illumination.

Dye/Cell	**Electrolyte**	**CDCA / dye**	**CDCA / electrolyte**	**J_{sc} (mA/cm^2)**	**V_{oc} (mV)**	**FF**	**η (%)**
Z907-I-1	I$^-$/I$_3^-$	No	No	13.0	780	0.64	6.5
Z907-I-2	I$^-$/I$_3^-$	0.02 M	0.01 M	12.3	780	0.69	6.6
Z907-terpy-1	Cobalt	No	No	1.7	572	0.48	0.5
Z907-terpy-2	Cobalt	0.02 M	0.01 M	4.5	635	0.47	1.3

Z907-bpy-TFSI	Cobalt	0.02 M	0.01 M	6.1	668	0.53	2.2
Z907-bpy-PF_6	Cobalt	0.02 M	0.01 M	9.4	764	0.63	4.5
N719-I-1	I^-/I_3^-	No	No	14.0	758	0.64	6.8
N719-I-2	I^-/I_3^-	0.02 M	0.01 M	13.2	780	0.67	6.9
N719-terpy-1	Cobalt	No	No	2.1	574	0.50	0.6
N719-terpy-2	Cobalt	0.02 M	0.01 M	2.7	626	0.58	1.0
N719-bpy-TFSI	Cobalt	0.02 M	0.01 M	4.1	638	0.54	1.4
N719-bpy- PF_6	Cobalt	0.02 M	0.01 M	6.6	656	0.60	2.6

Figure 3. JV characteristic of (a) Z907 terpy-1 (black line), Z907 terpy-2 (red line), Z907 bpy-TFSI (blue line) and Z907 bpy-PF_6 (green line); (b) N719 terpy-1 (black line), N719 terpy-2 (red line), N719 bpy-TFSI (blue line) and N719 bpy-PF_6 (green line).

For the new $[Co(Cl\text{-}phen\text{-}terpy)_2]^{2+/3+}$ electrolyte, quite poor performances were obtained when no CDCA was used (Z907-terpy-1 and N719-terpy-1). The concomitant use of CDCA both in dye bath and electrolyte solution leads in both cases to a strong improvement of the devices efficiency, by about a factor 2, as already demonstrated for the $[Co(bpy)_3]^{2+/3+}$ based electrolyte,[46] due to a concomitant gain in J_{sc} and V_{oc} (Z907-terpy-2 and N719-terpy-2). In this condition, better performances were obtained by using the Z907 dye for all the tested electrolytes, probably due to the synergic effect in shielding the TiO_2 surface from the oxidized form of the redox couples by both the coadsorbed CDCA and the dye alkyl chains, limiting the recombination processes.[46] On the other hand, addition of CDCA to the I^-/I_3^- electrolyte solution, having less recombination issues,[19] does not have a strong effect on the overall conversion efficiency (Z907-I-2 and N719-I-2). A slight decrease in the J_{sc} values is observed, probably due to the presence of adsorbed CDCA molecules on the TiO_2 surface, competing with the dye, compensated by an increase in the FF. A slight gain in the Voc for the N719-based devices (N719-I-2) is also observed, suggesting that a shielding effect is active also in this case. Although the overall effect of the CDCA use both in dye bath and in the electrolyte is an improvement of the photovoltaic performances, the obtained V_{oc} with the Co-based electrolytes remains lower than the corresponding values observed in the I^-/I_3^- based devices, without obtaining the expected gain on the basis of the measured redox potentials, due to the possibly different recombination kinetics between the redox shuttles.[46]

Moving to the comparison between the $[Co(Cl\text{-}phen\text{-}terpy)_2]^{2+/3+}$ and the $[Co(bpy)_3]^{2+/3+}$ based electrolytes, we note a similar trend with both the Z907 and the N719 dye. DSCs employing the $[Co(Cl\text{-}phen\text{-}terpy)_2]^{2+/3+}$ based electrolyte have lower efficiency with respect to the reference $[Co(bpy)_3]^{2+/3+}$ based devices. While the decrease in the V_{oc} values is not particularly marked and partly reflects the difference in the redox potential of the two redox shuttles, we observe a significant drop in the J_{sc}, by more than a factor 2 when compared to $[Co(bpy)_3](PF_6)_{2/3}$, which is the main cause of the lower efficiency. This problem could be attributable to different reasons, such as the higher competition of the terpyridine based redox mediator for the light absorption compared to the $[Co(bpy)_3]^{2+/3+}$ ones, or the charge recombination losses between the injected electrons and the oxidized form of the redox couple, leading to a decrease of the charge collection efficiency.[22] Moreover, the fact that also the fill factor values decrease moving from $[Co(Cl\text{-}phen\text{-}terpy)_2](TFSI)_{2/3}$ to $[Co(bpy)_3](TFSI)_{2/3}$ and $[Co(bpy)_3](PF_6)_{2/3}$ electrolytes, except for the N719-terpy-2 device, led us to think to mass transport limitations for the bulky $[Co(Cl\text{-}phen\text{-}terpy)_2]^{2+/3+}$ compared to the $[Co(bpy)_3]^{2+/3+}$ redox couple, as reported for the related substituted-bipyridine cobalt complexes.[22, 49, 56] To investigate this point, the $Co(Cl\text{-}phen\text{-}terpy)_2]^{2+/3+}$ based devices were measured under varying light intensities, see Table S1 in Supplementary Data. We observe quite a linear trend between the photocurrent values and the intensity of the incoming radiation in the investigated range, suggesting that in this case the diffusion of the redox couple is not the major issue limiting the photovoltaic performances. Thus, the reasons for the lower performance of Co(Cl-phen-terpy)$_2$]$^{2+/3+}$ based devices can be attributed to the decreased transparency of the electrolyte compared to the [Co(bpy)$_3$]$^{2+/3+}$ complexes and/or to the increased recombination between injected electrons and the cobalt(III) complex. As a matter of fact, by adding CDCA to the electrolyte solution, the photovoltaic performances increase by more than a factor 2 for the Co(Cl-phen-terpy)$_2$]$^{2+/3+}$ based devices, while a reduced performance increase is observed for the [Co(bpy)$_3$]$^{2+/3+}$ electrolyte. The reduced reorganization energy calculated for the Co(Cl-phen-terpy)$_2$]$^{2+/3+}$ electrolyte compared to [Co(bpy)$_3$]$^{2+/3+}$, which should speed-up dye regeneration, might however induce a higher propensity to recombination, as it was recently suggested by Kashif et al. for related pentadentate cobalt complexes.[55]

Regarding the effect of the counter-anion, the lower efficiency reported with the [Co(bpy)$_3$](TFSI)$_{2/3}$ with respect to the [Co(bpy)$_3$](PF$_6$)$_{2/3}$ is suggestive of a lower diffusion of the TFSI counter-anion in the electrolyte with respect to the PF$_6$, as previously reported.[49, 57]

4. Conclusions

A novel electrolyte [Co(Cl-phen-terpy)$_2$]$^{2+/3+}$ based on a substituted terpyridine ligand has been synthesized, characterized and tested in dye-sensitized solar cell devices, along with testing of electrolyte additives and of different counterions on the photovoltaic performances.

The [Co(Cl-phen-terpy)$_2$]$^{2+/3+}$ redox couple showed an oxidation potential of 0.47 V vs. NHE, i.e. slightly more positive than that of the standard the [Co(bpy)$_3$]$^{2+/3+}$ redox couple (0.56 V vs. NHE). The novel electrolyte delivered lower performances compared to the standard [Co(bpy)$_3$]$^{2+/3+}$ system carrying the same TFSI counterions, which in turn performed less efficiently than the same complex but carrying PF_6 counterions. The reasons for the lower performances are possibly due to parasitic recombination processes, lowering the photovoltage and the photocurrent of the devices, and to the limited diffusion of the TFSI counter-anion. Computational analyses provided oxidation potentials in good agreement with experimental values and suggested a lower reorganization for both the regeneration of the oxidized dye and the recombination with the oxidized electrolyte for a series of substituted terpyridine-based cobalt complexes, compared to the $[Co(bpy)_3]^{2+/3+}$ system. Thus although a faster regeneration of the oxidized dye could be expected this is most likely contrasted by the recombination losses and hindered by the slow mass transport of the bulky electrolyte. We have nevertheless demonstrated that simply by varying the composition of a cobalt-based electrolyte with the cheap and commercially available CDCA additive may further boost the efficiency of DSCs based on this redox mediator. Most notably, this effect is independent from the employed cobalt electrolyte.

Acknowledgement: We thank FP7-ENERGY-2011 project 261920, DST-EU' "ESCORT" for financial support.

Supplementary Data. ^{1}H-NMR and ^{19}F-NMR analysis of the $[Co(Cl\text{-}phen\text{-}terpy)_2](TFSI)_3$ and $[Co(bpy)_3](TFSI)_3$ complexes. Photovoltaic parameters of DSCs employing $[Co(Cl\text{-}phen\text{-}terpy)_2](TFSI)_{2/3}$ based electrolyte measured at low light intensities.

REFERENCES

[1] B. O'Regan, M. Grätzel, Nature 353 (1991) 737-740.
[2] M. Grätzel, Inorg. Chem. 44 (2005) 6841-6851.
[3] M. Grätzel, Nature 414 (2001) 338-344.
[4] M. Grätzel, Acc. Chem. Res. 42 (2009) 1788-1798.

[5] Y. Liu, J.R. Jennings, Y. Huang, Q. Wang, S.M. Zakeeruddin, M. Grätzel, J. Phys. Chem. C 115 (2011) 18847-18855.

[6] T. Daeneke, A.J. Mozer, Y. Uemura, S. Makuta, M. Fekete, Y. Tachibana, N. Koumura, U. Bach, L. Spiccia, J. Am. Chem. Soc. 134 (2012) 16925-16928.

[7] M.K. Nazeeruddin, P. Pèchy, T. Renouard, S.M. Zakeeruddin, R. Humphry-Baker, P. Comte, P. Liska, L. Cevey, E. Costa, V. Shklover, L. Spiccia, G.B. Deacon, C.A. Bignozzi, M. Grätzel, J. Am. Chem. Soc. 123 (2001) 1613-1624.

[8] P.G. Bomben, B.D. Koivisto, C.P. Berlinguette, Inorg. Chem. 49 (2010) 4960-4971.

[9] H.J. Snaith, A.J. Moule, C.d. Klein, K. Meerholz, R.H. Friend, M. Grätzel, Nano Lett. 7 (2007) 3372-3376.

[10] N. Cai, S.-J. Moon, L. Cevey-Ha, T. Moehl, R. Humphry-Baker, P. Wang, S.M. Zakeeruddin, M. Grätzel, Nano Lett. 11 (2011) 1452-1456.

[11] A. Kojima, K. Teshima, Y. Shirai, T. Miyasaka, J. Am. Chem. Soc. 131 (2009) 6050-6051.

[12] M.M. Lee, J.l. Teuscher, T. Miyasaka, T.N. Murakami, H.J. Snaith, Science 338 (2012) 643-647.

[13] I. Chung, B. Lee, J. He, R.P.H. Chang, M.G. Kanatzidis, Nature 485 (2012) 486-489.

[14] L. Etgar, P. Gao, Z. Xue, Q. Peng, A.K. Chandiran, B. Liu, M.K. Nazeeruddin, M. Grätzel, J. Am. Chem. Soc. 134 (2012) 17396-17399.

[15] H.-S. Kim, C.-R. Lee, J.-H. Im, K.-B. Lee, T. Moehl, A. Marchioro, S.-J. Moon, R. Humphry-Baker, J.-H. Yum, J.E. Moser, M. Grätzel, N.-G. Park, Sci. Rep. 2 (2012).

[16] J.-H. Im, C.-R. Lee, J.-W. Lee, S.-W. Park, N.-G. Park, Nanoscale 3 (2011) 4088-4093.

[17] J.H. Noh, S.H. Im, J.H. Heo, T.N. Mandal, S.I. Seok, Nano Lett. 13 (2013) 1764-1769.

[18] J.M. Ball, M.M. Lee, A. Hey, H.J. Snaith, Energy Environ. Sci. (2013) http://dx.doi.org/10.1039/C1033EE40810H.

[19] G. Boschloo, A. Hagfeldt, Acc. Chem. Res. 42 (2009) 1819-1826.

[20] B.C. O'Regan, J.R. Durrant, Acc. Chem. Res. 42 (2009) 1799-1808.

[21] B.A. Gregg, F.o. Pichot, S. Ferrere, C.L. Fields, J. Phys. Chem. B 105 (2001) 1422-1429.

[22] S.M. Feldt, E.A. Gibson, E. Gabrielsson, L. Sun, G. Boschloo, A. Hagfeldt, J. Am. Chem. Soc. 132 (2010) 16714-16724.

[23] A. Yella, H.-W. Lee, H.N. Tsao, C. Yi, A.K. Chandiran, M.K. Nazeeruddin, E.W.-G. Diau, C.-Y. Yeh, S.M. Zakeeruddin, M. Grätzel, Science 334 (2011) 629-634.

[24] J.-H. Yum, E. Baranoff, F. Kessler, T. Moehl, S. Ahmad, T. Bessho, A. Marchioro, E. Ghadiri, J.-E. Moser, C. Yi, M.K. Nazeeruddin, M. Grätzel, Nat. Commun. 3 (2012) 631-638.

[25] H. Nusbaumer, J.-E. Moser, S.M. Zakeeruddin, M.K. Nazeeruddin, M. Grätzel, J. Phys. Chem. B 105 (2001) 10461-10464.

[26] S.A. Sapp, C.M. Elliott, C. Contado, S. Caramori, C.A. Bignozzi, J. Am. Chem. Soc. 124 (2002) 11215-11222.

[27] H. Nusbaumer, S.M. Zakeeruddin, J.-E. Moser, M. Grätzel, Chem. Eur. J. 9 (2003) 3756-3763.

[28] P.J. Cameron, L.M. Peter, S.M. Zakeeruddin, M. Grätzel, Coord. Chem. Rev. 248 (2004) 1447-1453.

[29] H. Wang, P.G. Nicholson, L. Peter, S.M. Zakeeruddin, M. Grätzel, J. Phys. Chem. C 114 (2010) 14300-14306.

[30] S.M. Feldt, G. Wang, G. Boschloo, A. Hagfeldt, J. Phys. Chem. C 115 (2011) 21500-21507.

[31] H.N. Tsao , C. Yi , T. Moehl, J.-H. Yum, S.M. Zakeeruddin, M.K. Nazeeruddin, M. Grätzel, ChemSusChem 4 (2011) 591-594.

[32] T. Daeneke, T.-H. Kwon, A.B. Holmes, N.W. Duffy, U. Bach, L. Spiccia, Nat. Chem. 3 (2011) 1755-4330.

[33] T.W. Hamann, O.K. Farha, J.T. Hupp, J. Phys. Chem. C 112 (2008) 19756-19764.

[34] S.M. Feldt, U.B. Cappel, E.M.J. Johansson, G. Boschloo, A. Hagfeldt, J. Phys. Chem. C 114 (2010) 10551-10558.
[35] Y. Bai, Q. Yu, N. Cai, Y. Wang, M. Zhang, P. Wang, Chem. Commun. 47 (2011) 4376-4378.
[36] S. Hattori, Y. Wada, S. Yanagida, S. Fukuzumi, J. Am. Chem. Soc. 127 (2005) 9648-9654.
[37] Z. Zhang, P. Chen, T.N. Murakami, S.M. Zakeeruddin, M. Grätzel, Adv. Funct. Mater. 18 (2008) 341-346.
[38] M. Wang, N. Chamberland, L. Breau, J.-E. Moser, R. Humphry-Baker, B.t. Marsan, S.M. Zakeeruddin, M. Grätzel, Nat. Chem. 2 (2010) 385-389.
[39] B. O'Regan, D.T. Schwartz, Chem. Mater. 7 (1995) 1349-1354.
[40] B.C. O'Regan, F. Lenzmann, J. Phys. Chem. B 108 (2004) 4342-4350.
[41] V. Chakrapani, D. Baker, P.V. Kamat, J. Am. Chem. Soc. 133 (2011) 9607-9615.
[42] V. Jovanovski, V. Gonzàlez-Pedro, S. Gimènez, E. Azaceta, G.n. Cabañero, H. Grande, R. Tena-Zaera, I. Mora-Serò, J. Bisquert, J. Am. Chem. Soc. 133 (2011) 20156-20159.
- - , Q. Shen, T. Toyoda, J. Bisquert, Acc. Chem. Res. 42 (2009) 1848-1857.
[44] M.K. Nazeeruddin, F. De Angelis, S. Fantacci, A. Selloni, G. Viscardi, P. Liska, S. Ito, B. Takeru, M. Grätzel, J. Am. Chem. Soc. 127 (2005) 16835-16847.
[45] E. Mosconi, J.-H. Yum, F. Kessler, C.J. Gòmez Garcìa, C. Zuccaccia, A. Cinti, M.K. Nazeeruddin, M. Grätzel, F. De Angelis, J. Am. Chem. Soc. 134 (2012) 19438-19453.
[46] P. Salvatori, G. Marotta, A. Cinti, C. Anselmi, E. Mosconi, F. De Angelis, J. Phys. Chem. C 117 (2013) 3874-3887.
[47] M. Planells, F.J. Cespedes-Guirao, L. Goncalves, A. Sastre-Santos, F. Fernandez-Lazaro, E. Palomares, J. Mater. Chem. 19 (2009) 5818-5825.
[48] M. Planells, A. Gonzàlez, P. Ballester, E. Palomares, J. Porphyrins Phthalocyanines 15 (2011) 592-597.
[49] K.B. Aribia, T. Moehl, S.M. Zakeeruddin, M. Grätzel, Chem. Sci. 4 (2013) 454-459.
[50] A.D. Becke, J. Chem. Phys. 98 (1993) 5648-5652.
[51] M. Cossi, N. Rega, G. Scalmani, V. Barone, J. Comput. Chem. 24 (2003) 669-681.
[52] M.J. Frisch, G.W. Trucks, H.B. Schlegel, G.E. Scuseria, M.A. Robb, J.R. Cheeseman, J.A.J. Montgomery, T. Vreven, K.N. Kudin, J.C. Burant, J.M. Millam, S.S.T. Iyengar, J.; Barone, V.; Mennucci, B.; Cossi, M.; Scalmani, G.; Rega, N.; Petersson, G. A.; Nakatsuji, H.; Hada, M.; Ehara, M.; Toyota, K.; Fukuda, R.; Hasegawa, J.; Ishida, M.; Nakajima, T.; Honda, Y.; Kitao, O.; Nakai, H.; Klene, M.; Li, X.; Knox, J. E.; Hratchian, H. P.; Cross, J. B.; Bakken, V.; Adamo, C.; Jaramillo, J.; Gomperts, R.; Stratmann, R. E.; Yazyev, O.; Austin, A. J.; Cammi, R.; Pomelli, C.; Ochterski, J. W.; Ayala, P. Y.; Morokuma, K.; Voth, G. A.; Salvador, P.; Dannenberg, J. J.; Zakrzewski, V. G.; Dapprich, S.; Daniels, A. D.; Strain, M. C.; Farkas, O.; Malick, D. K.; Rabuck, A. D.; Raghavachari, K.; Foresman, J. B.; Ortiz, J. V.; Cui, Q.; Baboul, A. G.; Clifford, S.; Cioslowski, J.; Stefanov, B. B.; Liu, G.; Liashenko, A.; Piskorz, P.; Komaromi, I.; Martin, R. L.; Fox, D. J.; Keith, T.; Al-Laham, M. A.; Peng, C. Y.; Nanayakkara, A.; Challacombe, M.; Gill, P. M. W.; Johnson, B.; Chen, W.; Wong, M. W.; Gonzalez, C.; Pople, J. A., Gaussian, Inc., in, Wallingford CT, 2009.
[53] H. Torieda, K. Nozaki, A. Yoshimura, T. Ohno, J. Phys. Chem. A 108 (2004) 4819-4829.
[54] I. Krivokapic, M. Zerara, M.L. Daku, A. Vargas, C. Enachescu, C. Ambrus, P. Tregenna-Piggott, N. Amstutz, E. Krausz, A. Hauser, Coord. Chem. Rev. 251 (2007) 364-378.
[55] M.K. Kashif, J.C. Axelson, N.W. Duffy, C.M. Forsyth, C.J. Chang, J.R. Long, L. Spiccia, U. Bach, J. Am. Chem. Soc. 134 (2012) 16646-16653.
[56] J.J. Nelson, T.J. Amick, C.M. Elliott, The Journal of Physical Chemistry C 112 (2008) 18255-18263.
[57] S. Ahmad, T. Bessho, F. Kessler, E. Baranoff, J. Frey, C. Yi, M. Grätzel, M.K. Nazeeruddin, Phys. Chem. Chem. Phys. 14 (2012) 10631-10639.

Scheme1

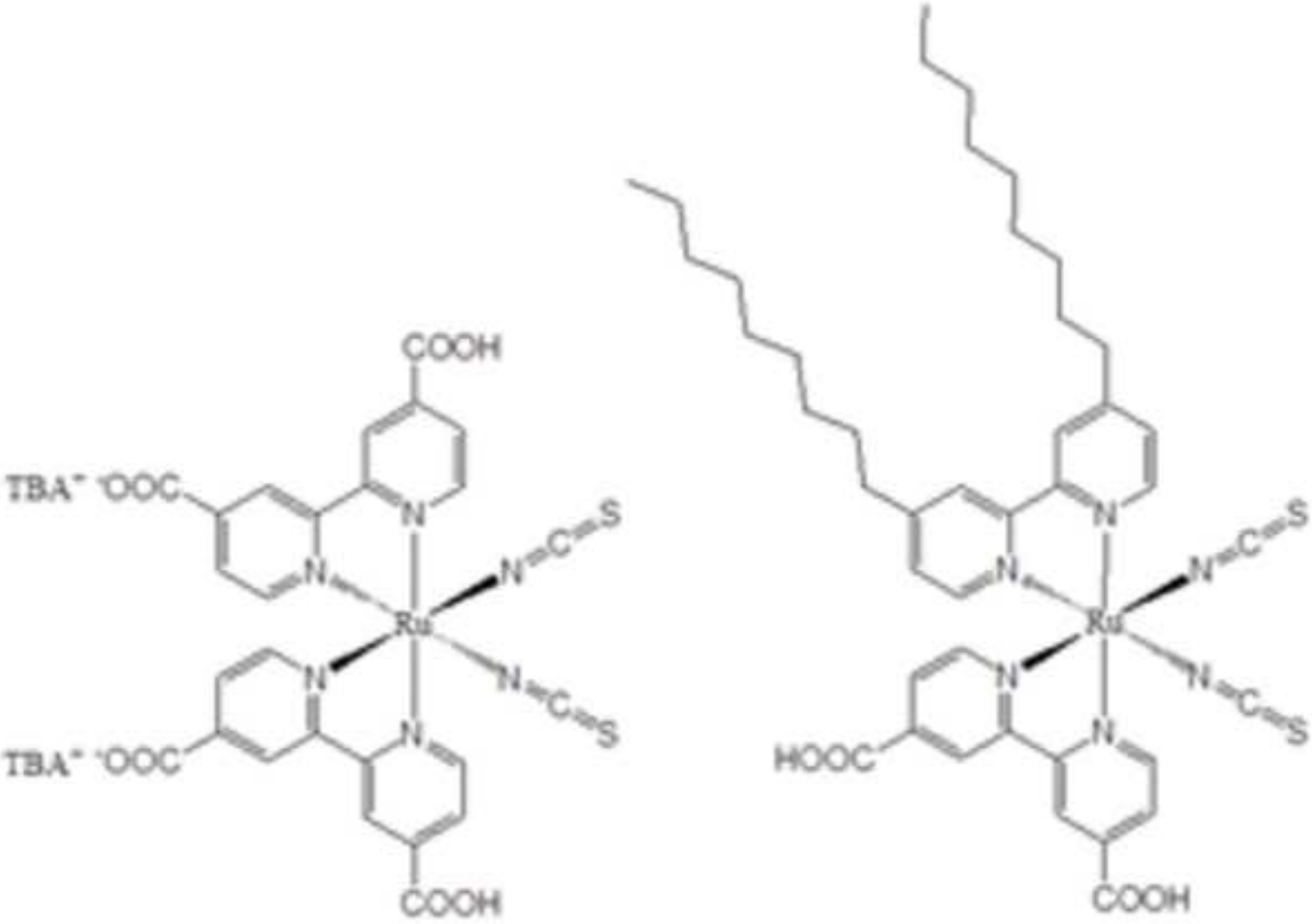

N719

Z907

Scheme2

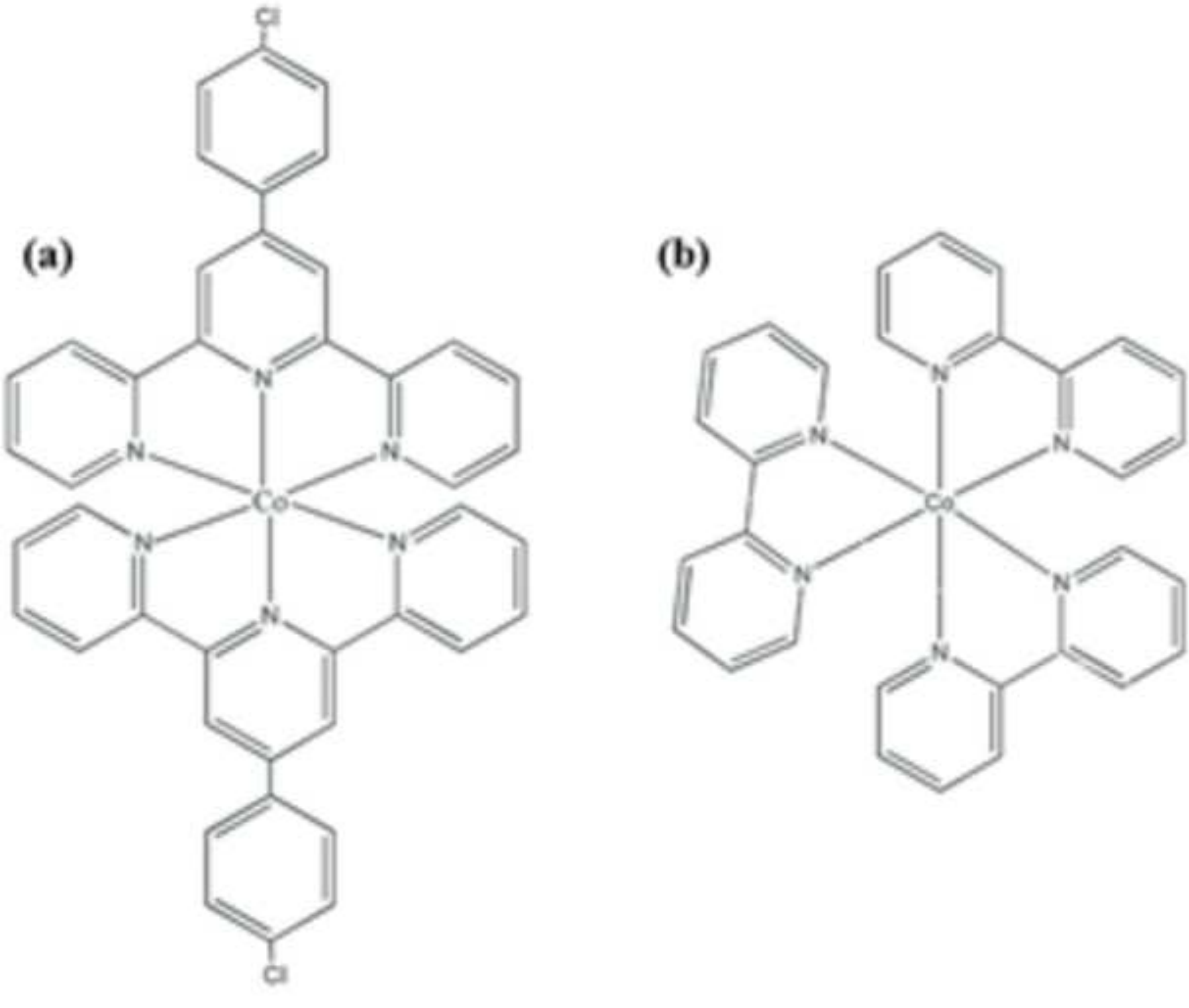

Figure1

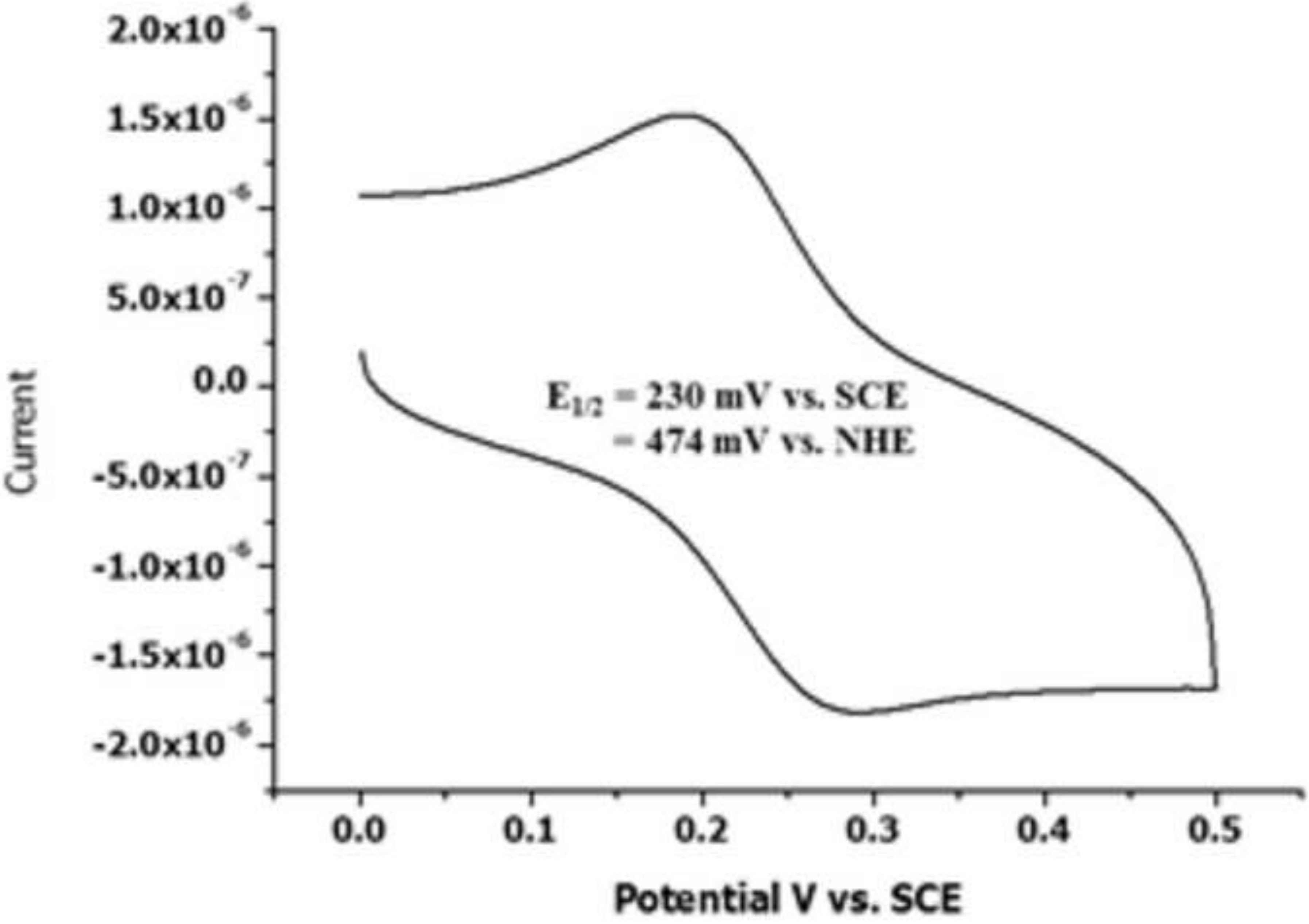
2.0x10^{-6}
1.5x10^{-6}
1.0x10^{-6}
5.0x10^{-7}
0.0
-5.0x10^{-7}
-1.0x10^{-6}
-1.5x10^{-6}
-2.0x10^{-6}
Current
$E_{1/2}$ = 230 mV vs. SCE
= 474 mV vs. NHE
0.0
0.1
0.2
0.3
0.4
0.5
Potential V vs. SCE

Figure2

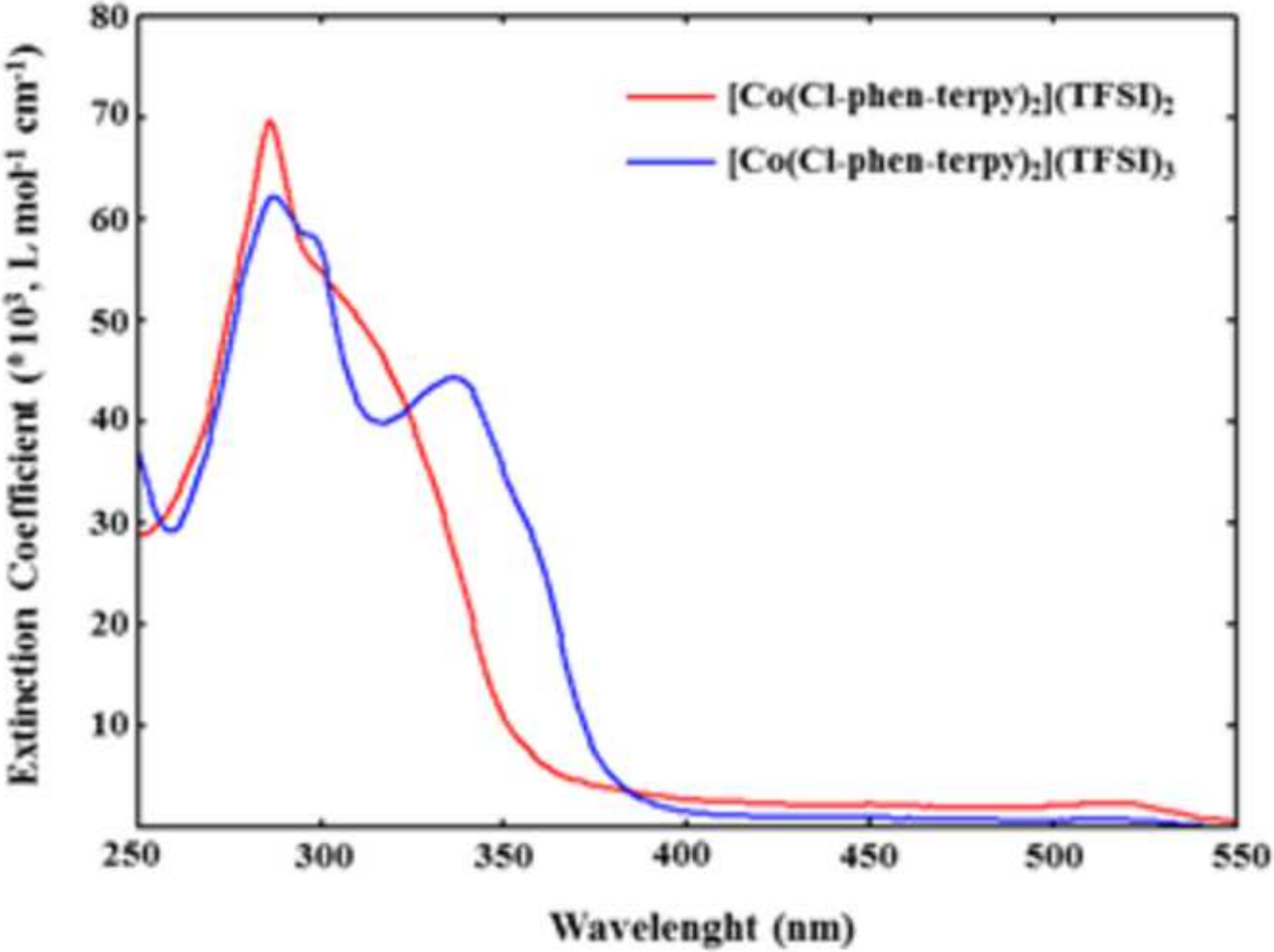

[Co(Cl-phen-terpy)$_2$](TFSI)$_2$
[Co(Cl-phen-terpy)$_2$](TFSI)$_3$
Extinction Coefficient (*10^3, L mol^{-1} cm^{-1})
80
70
60
50
40
30
20
10
250
300
350
400
450
500
550
Wavelenght (nm)

Figure 3

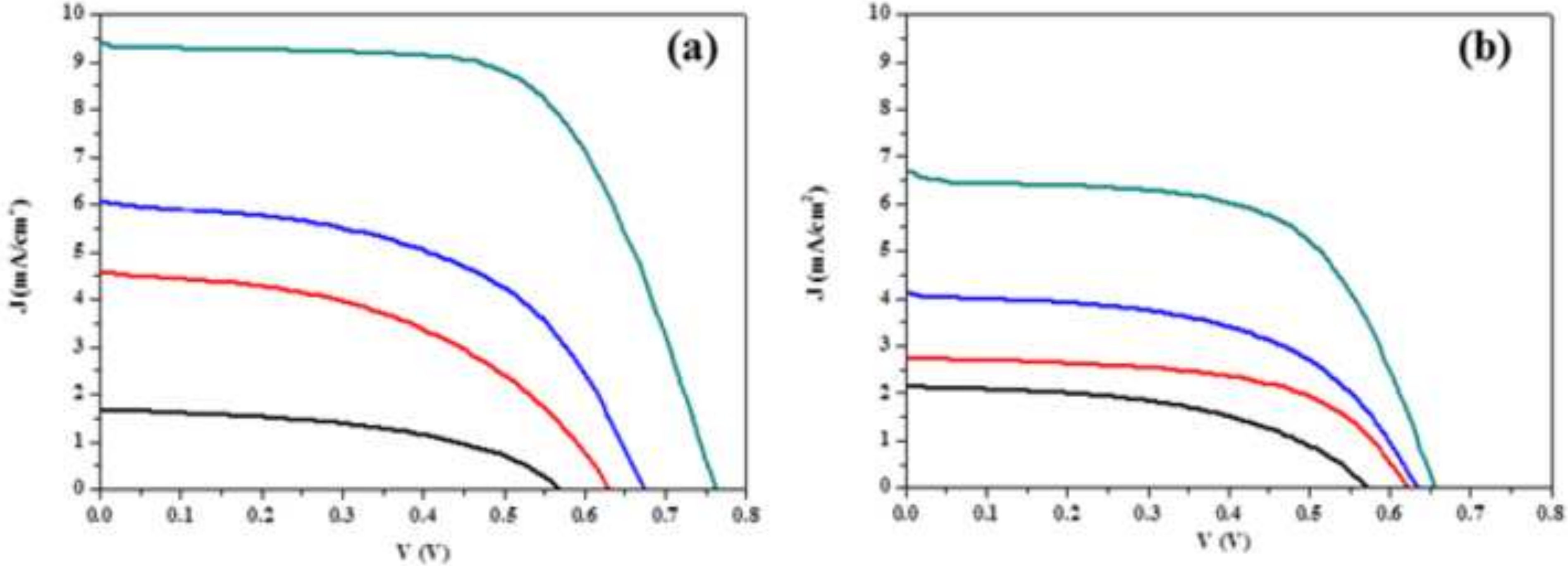

A new cobalt-terpyridine redox shuttle based on a substituted terpyridine ligand, has been synthesized, characterized, computationally investigated and tested in photovoltaic devices. The new redox shuttle is compared to the reference $[Co(bpy)_3]^{2+/3+}$, analyzing the effect of different counterions.

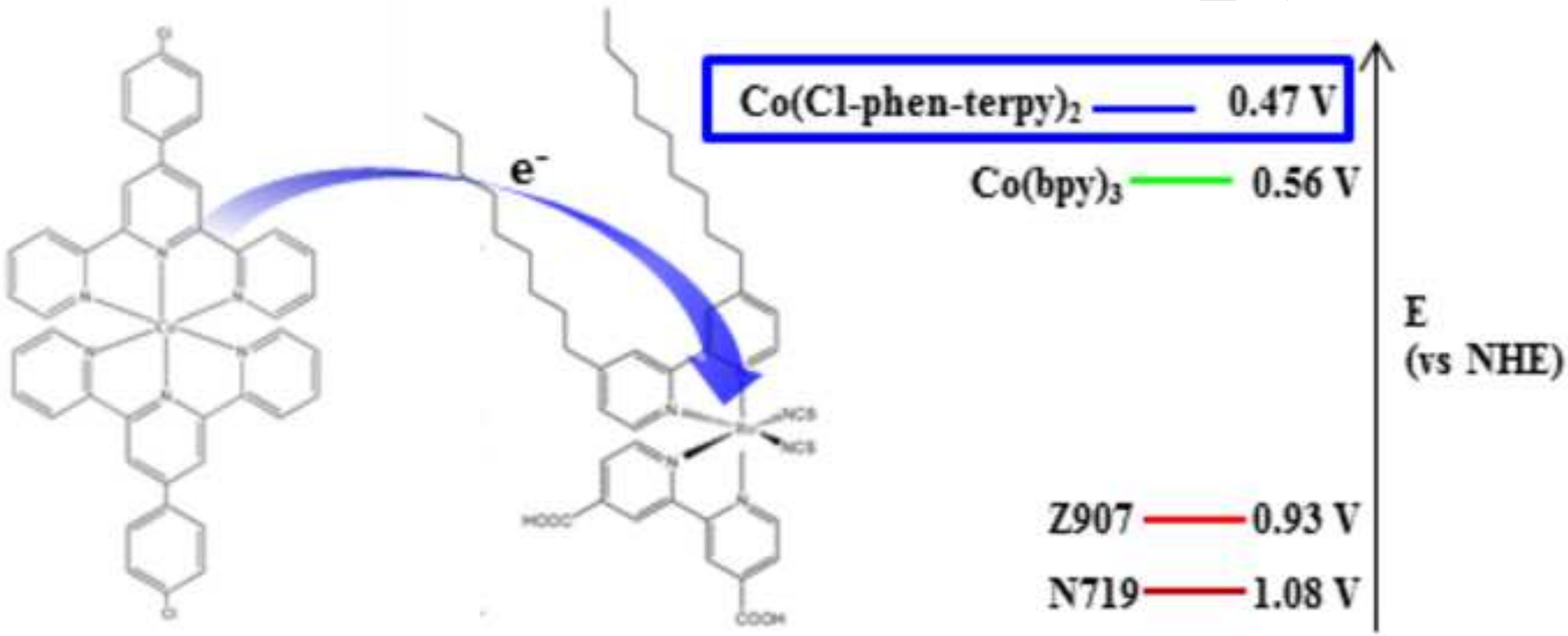
e-
Co(Cl-phen-terpy)₂ 0.47 V
Co(bpy)₃ 0.56 V
E
(vs NHE)
Z907 0.93 V
N719 1.08 V
NCS
NCS
HOOC
COOH
Cl
Cl

Highlights

- Synthesis and characterization of a [Co(Cl-phenyl-terpy)$_2$]$^{2+/3+}$ redox couple;
- Good agreement between experimental and calculated redox potentials;
- Photovoltaic efficiency compared to the [Co(bpy)$_3$]$^{2+/3+}$ electrolyte with different counterions;
- Improvement of the photovoltaic performances by using the CDCA additive.